



## Methanol Tolerance of Pd–Co Oxygen Reduction Reaction Electrocatalysts Using Scanning Electrochemical Microscopy

Cheng-Lan Lin, Carlos M. Sánchez-Sánchez, and Allen J. Bard<sup>\*,z</sup>

Center for Electrochemistry, Department of Chemistry and Biochemistry, University of Texas at Austin, Austin, Texas 78712, USA

Bimetallic Pd–Co and pure Pt electrocatalysts were evaluated for tolerance to methanol in the oxygen reduction reaction (ORR) in 0.5 M H<sub>2</sub>SO<sub>4</sub> using the tip generation–substrate collection mode of scanning electrochemical microscopy. The Pd–Co electrocatalyst, Pd<sub>80</sub>Co<sub>20</sub> (80% Pd, 20% Co), showed the highest ORR activity among the different Pd–Co compositions, both in the absence and presence of MeOH. The ORR collection efficiency of the electrocatalysts in electrolytes containing various MeOH concentrations were measured and compared, with the Pd<sub>80</sub>Co<sub>20</sub> electrocatalyst showing better tolerance toward MeOH poisoning during ORR than Pt electrocatalysts, especially at high MeOH concentrations.  
© 2008 The Electrochemical Society. [DOI: 10.1149/1.2931020] All rights reserved.

Manuscript submitted March 12, 2008; revised manuscript received April 29, 2008. Available electronically May 30, 2008.

The direct MeOH fuel cell (DMFC)<sup>1</sup> is a promising power source that possesses the advantages of a high theoretical energy density and the use of an easy-to-handle liquid fuel. However, DMFC performance is still far from the theoretical limit because of problems such as low efficiency and stability of the electrocatalysts and MeOH crossover through the proton-exchange membrane which can poison the oxygen reduction reaction (ORR) electrocatalysts.<sup>2,3</sup> Pt is the most studied and developed ORR cathode electrocatalyst for the DMFC, but its efficiency is degraded by the presence of MeOH in the electrolyte, which significantly reduces the performance of a DMFC.<sup>4</sup> Thus, there is interest in studying non-Pt-based ORR electrocatalysts and the MeOH effect on these, because they can offer a higher MeOH tolerance during the ORR.<sup>5–8</sup>

In our previous studies, the ORR activities of some bimetallic electrocatalysts in a MeOH-free solution were investigated using the tip generation–substrate collection (TG-SC) mode of the scanning electrochemical microscopy (SECM).<sup>9,10</sup> This imaging protocol, where oxygen is generated at the tip and reduced at the test electrocatalyst spot, provides high-throughput screening of the ORR activities of a wide range of electrocatalyst compositions. Among different bimetallic palladium-cobalt-based electrocatalysts tested, the Pd<sub>80</sub>Co<sub>20</sub> showed the highest ORR activity. For practical utilizations of the Pd<sub>80</sub>Co<sub>20</sub> in a DMFC, it is important to evaluate its MeOH tolerance for the ORR. Although some studies of the MeOH tolerance of Pd–Co catalysts<sup>11,12</sup> have been carried out using cyclic voltammetry, no quantitative data have been provided. Therefore, the present work is devoted to a quantitative study of the ORR electrocatalytic activities of Pd–Co mixtures in the presence of MeOH using the TG-SC mode of SECM. In particular, the MeOH tolerance of Pd<sub>80</sub>Co<sub>20</sub> as a function of applied potential was compared with that of a Pt electrocatalyst in the presence of various MeOH concentrations. This study provides a rapid and quantitative method to characterize the MeOH tolerance of these materials under steady-state conditions provided by the SECM. For this reason, the collection efficiency (CE), i.e., the amount of oxygen collected at the substrate as a function of potential, measured using SECM represents an accurate parameter to evaluate the performance of an electrocatalyst.

### Experimental

**General.**— Glassy carbon (GC) plates (Alfa Aesar, Ward Hill, MA, 1 mm thick) were cut into 16 × 16 mm squares prior to use. H<sub>2</sub>PdCl<sub>4</sub> (99.998%, Alfa Aesar, Ward Hill, MA), Co(NO<sub>3</sub>)<sub>2</sub>·6H<sub>2</sub>O (99.999%, Alfa Aesar, Ward Hill, MA), and sulfuric acid (trace metal, Fisher Scientific, Canada) were all reagent grade and were used as received. Milli-Q water was used in all experiments. Elec-

trochemical experiments were carried out using an SECM CHI 900B (CHI Instruments, Austin, TX) with a gold wire as the counter electrode. A homemade reversible hydrogen electrode (RHE) was used as the reference electrode. Before each experiment, a Pt wire (0.5 mm diameter) was assembled in a glass tube with a frit at its terminal and filled with 0.5 M sulfuric acid solution. By applying a negative potential (–2.0 V vs Ag/AgCl) to the Pt wire, a hydrogen bubble was generated and maintained contact with the Pt wire. This arrangement produces an electrode that is close to that of a standard hydrogen electrode. The potential of our RHE was stable during the entire experimental time period, and all potentials in the text are referenced to it.

**Pd–Co array preparation.**— A series of Pd–Co mixture spots with different Pd-to-Co ratios were prepared on a GC substrate as described previously.<sup>9</sup> Briefly, solutions with 0.3 M Pd(II) and 0.3 M Co(II) in water–glycerol (volume ratio = 3:1) solutions were used as the precursors for the preparation of Pd–Co mixtures. A picoliter solution dispenser (CHI mode 1550, Austin, TX) was employed to deposit the precursor solutions successively onto a GC substrate to form an array of spots containing different volume ratios of the precursors. The as-prepared array was dried under Ar at 150°C overnight and then reduced under H<sub>2</sub> at 350°C for 1 h in a tube furnace. The average diameters of the final spots were about 225 μm.

**Ultramicroelectrode preparation.**— Au (25 μm diameter) and Pt (100 μm diameter) tips were fabricated by heat-sealing the corresponding metal wire under vacuum in a borosilicate glass capillary.<sup>13</sup> Sandpaper was used to remove the bottom cross section of glass to reveal the metal disk, and the metal surfaces were polished sequentially with different-sized alumina oxide powder (from 1.0 to 0.3 to 0.05 μm).

**Cyclic voltammograms.**— A conventional three-electrode system was employed for cyclic voltammetry experiments. The reference electrode was a RHE, and a gold wire was used as the counter electrode. Electrolytes were purged with Ar for at least 15 min before each experiment. The scan rate was 100 mV s<sup>–1</sup>.

**SECM images of the Pd–Co array.**— The images were acquired using the TG-SC mode of SECM. The electrolytes were aq. 0.5 M sulfuric acid with or without 0.5 M MeOH and were Ar purged for at least 15 min before imaging to remove the oxygen in the solutions. An Ar blanket was kept above the electrolyte throughout the imaging processes. Au has negligible catalytic activity toward MeOH oxidation in bulk form;<sup>14</sup> for this reason, a Au ultramicroelectrode (UME) tip (diameter = 25 μm) served as an oxygen generator. The use of gold as a tip material and as a counter electrode also eliminates the possibility of contamination of the electrocatalyst by small amounts of dissolved Pt. A constant oxidative current

\* Electrochemical Society Fellow.

<sup>z</sup> E-mail: ajbard@mail.utexas.edu

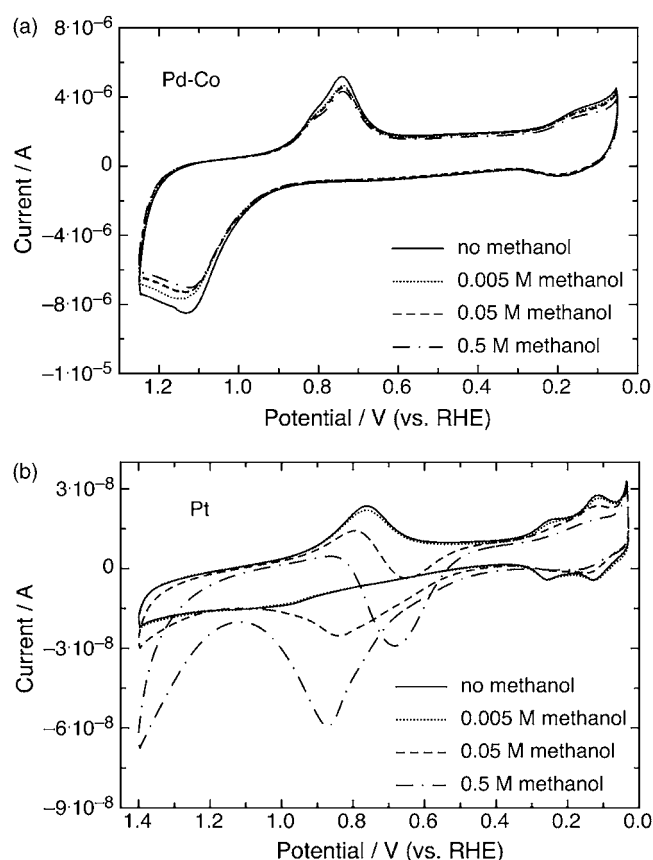


**Figure 1.** Cyclic voltammograms of (a) a Pd-Co array and (b) a Pt UME (diameter = 100  $\mu\text{m}$ ) in a deaerated 0.5 M sulfuric acid solution containing different MeOH concentrations. The scan rate was 100 mV/s.

( $-155$  nA) was applied to the gold UME tip by an external 9 V battery connected to a gold counter electrode. The tip was scanned in the  $X$ - $Y$  plane over the Pd-Co array substrate at a constant tip-substrate distance of 45  $\mu\text{m}$ . During the scan the gold tip generated  $\text{O}_2$  at a constant current, and the entire array was held at a constant potential where the ORR could take place.

**ORR CE of an electrocatalytic spot.**—The ORR CE of a  $\text{Pd}_{80}\text{Co}_{20}$  spot on GC and a Pt tip (diameter = 100  $\mu\text{m}$ ) in electrolytes with different MeOH concentrations were estimated by steady-state TG-SC measurements.<sup>15,16</sup> According to previously reported calibration data for the TG-SC mode of SECM,<sup>17</sup> 100% CE is achievable when the tip-substrate distance is smaller than 10  $\mu\text{m}$ . For this reason, the oxygen generator tip was placed at 7  $\mu\text{m}$  above the center of the spot for CE measurements. Initially, the substrate was held at a constant potential while the oxygen generator tip was turned off. When a steady-state substrate current was recorded, the oxygen generator tip was turned on and a constant oxygen flux was generated for 90 s. The corresponding current response of the  $\text{Pd}_{80}\text{Co}_{20}$  spot or the Pt UME was recorded. To clean and restore the electrocatalyst surface, two cyclic voltammetric scans between 0.05 and 1.40 V were performed before each measurement.

### Results and Discussion

Cyclic voltammograms of a Pd-Co array and a Pt UME in electrolytes containing different MeOH concentrations are shown in Fig. 1. Pt is a good electrocatalyst for the ORR and also for MeOH oxidation,<sup>2,3</sup> and for this reason it was employed as a comparison standard. Figure 1b shows a MeOH oxidation peak with a peak potential at 0.85 V and the onset potential around 0.50 V when Pt is used as the electrode. Larger peak currents are observed when

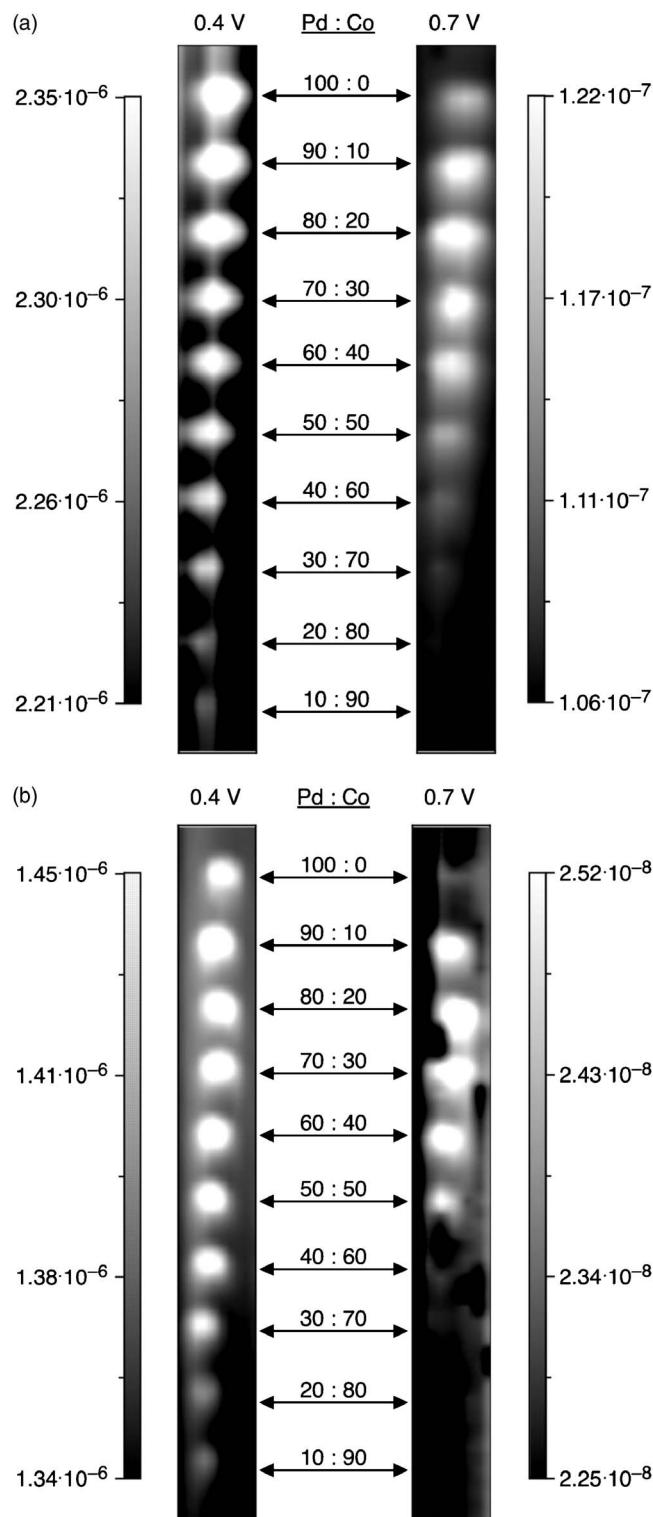


**Figure 2.** SECM TG-SC images of ORR activities measured on a Pd-Co array at 0.4 and 0.7 V in 0.5 M sulfuric acid solution in (a) the absence or (b) the presence of 0.5 M MeOH in solution. The distance between the tip and the GC substrate was 45  $\mu\text{m}$ , and the oxygen was generated at a constant current of  $-155$  nA. The scan rate was 25  $\mu\text{m}$  each 0.2 s. The scale bars in the figures are the current ranges in A.

higher MeOH concentrations are present in the electrolytes. Note that Pt exhibits ORR activity in the same potential range as the MeOH oxidation reaction; therefore, they are competitive reactions. Moreover, Fig. 1b shows that hydrogen adsorption peaks become

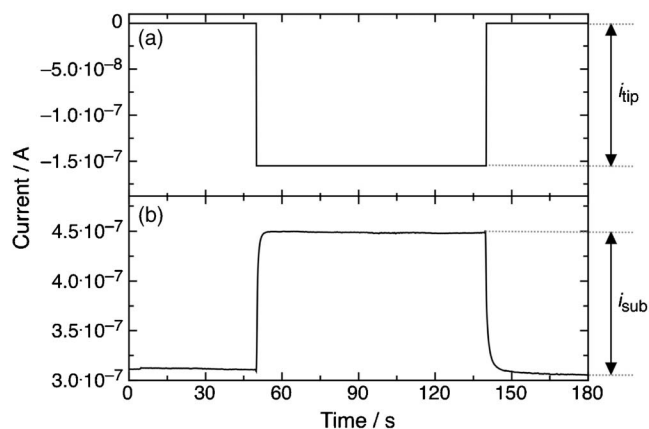


**Figure 3.** (a) Typical current profile of oxygen generation at the tip ( $i_{\text{tip}}$ ), and (b) the corresponding ORR current response at a  $\text{Pd}_{80}\text{Co}_{20}$  spot below the tip ( $i_{\text{sub}}$ ) in a TG-SC experiment. The distance between the oxygen generator tip and the  $\text{Pd}_{80}\text{Co}_{20}$  spot was  $7 \mu\text{m}$ . The ORR was carried out at  $0.4 \text{ V}$  in a  $0.5 \text{ M}$  sulfuric acid solution containing  $0.5 \text{ M}$  MeOH.

smaller with an increase of MeOH concentration, probably because of the adsorption of MeOH or some intermediates generated during MeOH oxidation on the Pt electrode surface that block hydrogen adsorption sites. In contrast, no obvious MeOH oxidation current response can be observed on the Pd-Co electrocatalyst array before the oxidation of Pd ( $E \leq 0.9 \text{ V}$ ) for all MeOH concentrations studied (Fig. 1a). However, the oxidation peak current between  $1.0$  and  $1.2 \text{ V}$  decreases with increasing MeOH concentration, again because of possible adsorption of either MeOH or intermediates generated from MeOH oxidation on the electrocatalyst surface. These voltammograms suggest that the Pd-Co electrocatalysts have much poorer activity toward MeOH oxidation than Pt. Therefore, Pd-Co electrocatalysts exhibit better resistances against MeOH poisoning during ORR than Pt as well.

SECM images of ORR activity of a Pd-Co array in the absence or the presence of  $0.5 \text{ M}$  MeOH at  $0.4$  and  $0.7 \text{ V}$  were obtained using the TG-SC mode of SECM (Fig. 2). A Pd-Co array was placed in a deaerated  $0.5 \text{ M}$  sulfuric acid solution with or without  $0.5 \text{ M}$  MeOH, while an oxygen generator tip was scanned above the array. The tip-generated oxygen was reduced at the Pd-Co array, and the ORR activity of each electrocatalyst spot was recorded in terms of their current responses. As shown in Fig. 2a and b, both images show higher ORR activities at the Pd-rich spots, although smaller currents were recorded when the electrolyte contained MeOH. Similar ORR activities were observed for the Pd-Co electrocatalysts, with Pd compositions ranging from  $70$  to  $100\%$  at

$0.4 \text{ V}$  in both images, respectively. But, when the ORR was carried out with the substrate at  $0.7 \text{ V}$ , the  $\text{Pd}_{80}\text{Co}_{20}$  spot showed higher activities than other compositions in both electrolytes with and without  $0.5 \text{ M}$  MeOH. For DMFC applications, it is desirable to operate the ORR cathode electrocatalysts at as positive potential as possible to increase the overall cell voltage. Therefore,  $\text{Pd}_{80}\text{Co}_{20}$  shows promising ORR activity in the presence of high MeOH concentration.

To quantitatively compare the MeOH tolerance of the  $\text{Pd}_{80}\text{Co}_{20}$  electrocatalyst to a Pt electrocatalyst, the CE of these ORR electrocatalysts at different working potentials in electrolytes with various MeOH concentrations was evaluated by a steady-state TG-SC method.<sup>15,16</sup> The CE is defined as the percentage of the oxygen generated at a tip that is being reduced by an electrocatalyst and can be expressed as

$$CE(\%) = \left| \frac{i_{\text{sub}}}{i_{\text{tip}}} \right| \times 100\%$$

when the spacing,  $d$ , between tip and substrate is small, where  $i_{\text{tip}}$  is the current applied to the oxygen generator tip and  $i_{\text{sub}}$  is the corresponding current response of the electrocatalyst substrate. Oxygen was generated by applying a constant oxidative current to a gold UME tip at a close distance above an electrocatalyst spot. A typical current-time profile for oxygen generation at the tip and the corresponding ORR current response at the  $\text{Pd}_{80}\text{Co}_{20}$  electrocatalyst is shown in Fig. 3. Figure 4 shows the ORR CE of a  $\text{Pd}_{80}\text{Co}_{20}$  spot and a Pt UME in the presence of different MeOH concentrations as a function of the working potential, respectively. The  $\text{Pd}_{80}\text{Co}_{20}$  electrocatalyst shows slightly lower, but comparable, ORR activity to Pt in the absence of MeOH in the electrolyte. However, while the CEs of Pt gradually dropped in the presence of increasing amounts of MeOH in the electrolyte (from  $0.005$  to  $0.05 \text{ M}$ ), the CEs of  $\text{Pd}_{80}\text{Co}_{20}$  remained essentially constant, and only large amounts of MeOH ( $0.5 \text{ M}$ ) produced a clear poisoning effect. Note that the CE of  $\text{Pd}_{80}\text{Co}_{20}$  was significantly higher than that of Pt when  $0.5 \text{ M}$  MeOH was present in the solution. For example, the  $\text{Pd}_{80}\text{Co}_{20}$  at  $0.8 \text{ V}$  showed a CE value of  $36\%$ , which is about  $3.5$  times higher than that of Pt in the presence of  $0.5 \text{ M}$  MeOH. Therefore, based on the ORR CE measurements, the  $\text{Pd}_{80}\text{Co}_{20}$  electrocatalyst exhibits higher MeOH tolerance than Pt during ORR.

## Conclusions

This study provides an alternative method using SECM for rapid and quantitative characterization of the MeOH tolerance of new ORR electrocatalysts. From the results of cyclic voltammetry, SECM TG-SC images, and CE measurements, we conclude that the  $\text{Pd}_{80}\text{Co}_{20}$  electrocatalyst shows better MeOH tolerance than Pt dur-

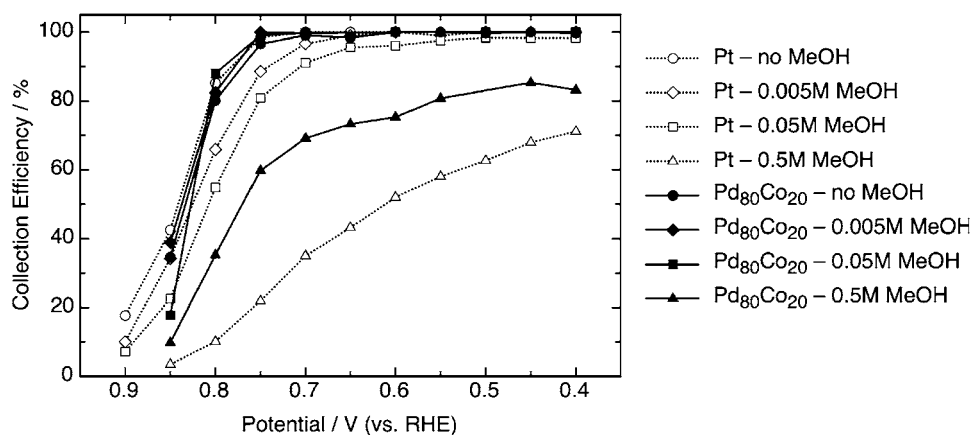


**Figure 4.** ORR CE of a  $\text{Pd}_{80}\text{Co}_{20}$  spot and a Pt UME (diameter  $100 \mu\text{m}$ ) as a function of the working potential in  $0.5 \text{ M}$  sulfuric acid solution containing different MeOH concentrations.

ing ORR, especially in the presence of a high MeOH concentration, and therefore is a good candidate material for the cathode electrocatalyst in DMFCs.

#### Acknowledgments

This work has been supported by MURI [DoD - Office of Naval Research (N00014-07-1-0758)]. C. M. Sánchez-Sánchez thanks the Ministerio Español de Educación y Ciencia and Fundacion Española para la Ciencia y la Tecnología for a postdoctoral fellowship.

#### References

1. G. J. K. Acres, *J. Power Sources*, **100**, 60 (2001).
2. S. Wasmus and A. Küver, *J. Electroanal. Chem.*, **461**, 14 (1999).
3. A. S. Aricò, S. Srinivasan, and V. Antonucci, *Fuel Cells*, **1**, 133 (2001).
4. M. K. Ravikumar and A. K. Shukla, *J. Electrochem. Soc.*, **143**, 2601 (1996).
5. R. W. Reeve, P. A. Christensen, A. Hamnett, S. A. Haydock, and S. C. Roy, *J. Electrochem. Soc.*, **145**, 3463 (1998).
6. J.-F. Drillet, A. Ee, J. Friedemann, R. Kotz, B. Schnyder, and V. M. Schmidt, *Electrochim. Acta*, **47**, 1983 (2002).
7. J.-G. Oh, C.-H. Lee, and H. Kim, *Electrochem. Commun.*, **9**, 2629 (2007).
8. K. Lee, L. Zhang, and J. Zhang, *J. Power Sources*, **170**, 291 (2007).
9. J. L. Fernández, D. A. Walsh, and A. J. Bard, *J. Am. Chem. Soc.*, **127**, 357 (2005).
10. J. L. Fernández, J. M. White, Y. Sun, W. Tang, G. Henkelman, and A. J. Bard, *Langmuir*, **22**, 10426 (2006).
11. W. Wang, D. Zheng, C. Du, Z. Zou, X. Zhang, B. Xia, H. Yang, and D. L. Akins, *J. Power Sources*, **167**, 243 (2007).
12. L. Zhang, K. Lee, and J. Zhang, *Electrochim. Acta*, **52**, 3088 (2007).
13. A. J. Bard and M. V. Mirkin, *Scanning Electrochemical Microscopy*, Marcel Dekker, New York (2001).
14. M. Haruta, *Catal. Today*, **36**, 153 (1997).
15. J. L. Fernández and A. J. Bard, *Anal. Chem.*, **75**, 2967 (2003).
16. J. L. Fernández and A. J. Bard, *Anal. Chem.*, **76**, 2281 (2004).
17. P. R. Unwin and A. J. Bard, *J. Phys. Chem.*, **96**, 5035 (1992).